Transformations of high spin Mn^{II} and Fe^{II} polymeric pivalates in reactions with pivalic acid and *o*-phenylenediamines

M. A. Kiskin,[a]★ G. G. Aleksandrov,[a] Zh. V. Dobrokhotova,[a] V. M. Novotortsev,[a] Yu. G. Shvedenkov,[b] and I. L. Eremenko[a]

[a]*N. S. Kurnakov Institute of General and Inorganic Chemistry, Russian Academy of Sciences, 31 Leninsky prosp., 119991 Moscow, Russian Federation. Fax: +7 (495) 955 4835. E-mail: ilerem@igic.ras.ru*

[b]*A. V. Nikolaev Institute of Inorganic Chemistry, Siberian Branch, Russian Academy of Sciences, 3 prosp. Akad. Lavrent´eva, 630090 Novosibirsk, Russian Federation. Fax: +7 (383) 330 9489*

The thermolysis and reactions of the polymeric high spin Mn^{II} and Fe^{II} complexes $[Mn(\mu\text{-}OOCBu^t)_2(HOEt)]_n$ (**1**) and $[Fe(\mu\text{-}OOCBu^t)_2]_n$ (**3**) with pivalic acid and *o*-phenylenediamines 1,2-$(NH_2)_2C_6H_2R_2$ (R = H or Me) were studied. The synthesis of compound **1** performed with a deficiency of pivalate anions affords the antiferromagnetic chloropivalate polymer $\{(MeCN)(HOOCBu^t)(H_2O)Mn_5Cl(OH)(OOCBu^t)_8 \cdot MeCN\}_n$. The reaction of **1** with an excess of pivalic acid produces the antiferromagnetic polymer $[Mn_4(OOCBu^t)_8(HOOCBu^t)_2]_n$. The analogous reaction of pivalic acid with polymer **3** gives the mononuclear complex $Fe(\eta^1\text{-}OOCBu^t)_2(\eta^1\text{-}HOOCBu^t)_4$ containing the high spin iron(II) atom as the major product. Study of the reactions of **3** with a deficiency (<1 : 1) and an excess (>1 : 1) of diamines demonstrated that the polymer $\{[(\eta^2\text{-}(NH_2)_2C_6H_4)_2Fe(\mu\text{-}OOCBu^t)_2][Fe_2(\mu\text{-}OOCBu^t)_4] \cdot 2MeCN\}_n$ is generated as the major product in the former case, whereas the mononuclear complexes $Fe(\eta^1\text{-}OOCBu^t)_2[\eta^1\text{-}(NH_2)_2C_6H_4]_4$ and $Fe(\eta^1\text{-}OOCBu^t)_2[\eta^2\text{-}(NH_2)_2C_6H_2Me_2][\eta^1\text{-}(NH_2)_2C_6H_2Me_2]_2$ are predominantly obtained in the latter case.

Key words: iron(II) complexes, polynuclear manganese(II) complexes, carboxylate ligands, synthesis, X-ray diffraction study, magnetic properties, thermal decomposition.

In the synthesis of molecular magnets, it is important to correctly choose the starting compound containing high spin transition metal ions. Coordination polymers are convenient compounds because their directed chemical degradation allows one to form molecules with desired structures and, as a result, with a particular spin density distribution.[1—5] The number of metal centers and the mutual arrangement of magnetic ions in the newly formed molecules are determined by the electronic nature and structural characteristics of the donor organic ligands used as "slicers" for such *n*-dimensional systems.

Recently, we have found that the polymeric carboxylate complexes $[M(\mu\text{-}OOCBu^t)_2(HOEt)]_n$ (**1** and **2**) (M = Mn^{II} (**1**) or Fe^{II} (**2**)) and $[Fe(\mu\text{-}OOCBu^t)_2]_n$ (**3**) are transformed in nearly 100% yield into dinuclear antiferromagnets $L_2M_2(\mu\text{-}OOCBu^t)_4$ (M = Mn, L is 2,6-diaminopyridine; M = Fe, L is 2,6-lutidine or 2,6-diaminopyridine)[6—8] with high spin Mn^{II} (S = 5/2)[9] and Fe^{II} (S = 2)[10] atoms by the reactions with α-substituted pyridines. In the present study, we examined the reactions of Mn^{II} and Fe^{II} polymeric pivalates with *O*- and *N*-donor organic molecules containing two donor centers, in particular, with pivalic acid and *o*-phenylenediamines 1,2-$(NH_2)_2C_6H_2R_2$ (R = H or Me). We also studied the thermolysis products of these polymers. These investigations are also of interest because the starting polymeric "spin materials" differ in the magnetic characteristics. Iron derivatives **2** and **3** exhibit the ferromagnetic properties unlike antiferromagnetic manganese polymer **1**. Moreover, magnetic ordering was observed for complex **3** at 3.8 K (Fig. 1).

Results and Discussion

Earlier,[6] we have demonstrated that the coordination polymer $[Mn(\mu\text{-}OOCBu^t)_2(HOEt)]_n$ (**1**) readily soluble in organic solvents can easily be prepared in high yield by the reaction of manganese(II) salts with potassium pivalate ($KOOCBu^t$) in ethanol. However, it appeared that it is important to use a special reagent ratio in the synthesis of **1**. When pivalate anions are in deficiency, the reaction of aqueous manganese chloride with $KOOCBu^t$ (reagent ratio [Mn] : [K] ≈ 1.5 : 2) produces a polymeric complex containing the MnCl fragments incor-

Published in Russian in *Izvestiya Akademii Nauk. Seriya Khimicheskaya,* No. 5, pp. 779—792, May, 2006.

1066-5285/06/5505-0806

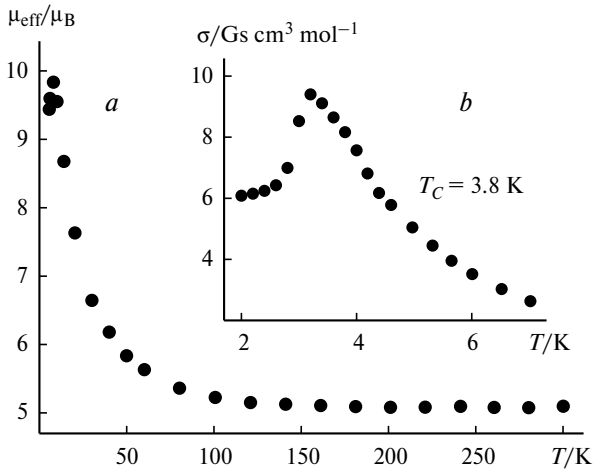

Fig. 1. Plots of $\mu_{eff}(T)$ (*a*) and magnetization $\sigma(T)$ measured in a small magnetic field (*b*) for complex **3**.

porated into the polymer system of manganese pivalate. Recrystallization of this product from acetonitrile afforded the polymeric compound $\{(MeCN)(HOOCBu^t)(H_2O)Mn_5Cl(OH)(OOCBu^t)_8 \cdot \cdot MeCN\}_n$ (**4**) in 46% yield (Scheme 1).

X-ray diffraction study demonstrated that polymer **4** is a complex chain consisting of the pentanuclear fragments $(MeCN)(HOOCBu^t)(H_2O)Mn_5Cl(OH)(OOCBu^t)_8$. Each fragment contains the triangle of manganese atoms centered by the bridging hydroxy group, $Mn_3(\mu_3\text{-}OH)$, as the central unit (Mn—O, 2.103(8)—2.150(8) Å). Two of three Mn atoms of this triangle (Mn...Mn, 3.505(3) Å) are linked together by two *O*,*O*-bridging carboxylate

Scheme 1

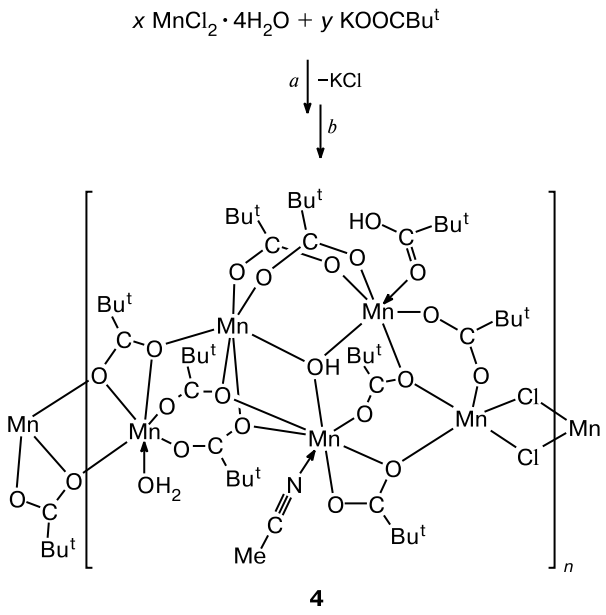

Reagents and conditions: *a*. $1.5 < x : y < 2$, EtOH, Ar, 87 °C; *b*. MeCN, Ar, 81 °C.

groups (Mn—O, 2.094(8)—2.213(9) Å), whereas the third Mn atom is linked to the other two Mn atoms by one *O*,*O*-carboxylate bridge (Mn...Mn, 3.626(3) Å; Mn—O, 2.099(9), 2.326(9) Å) and one *O*-carboxylate bridge (Mn...Mn, 3.370(3) Å; Mn—O, 2.142(9), 2.323(8) Å) (Fig. 2).

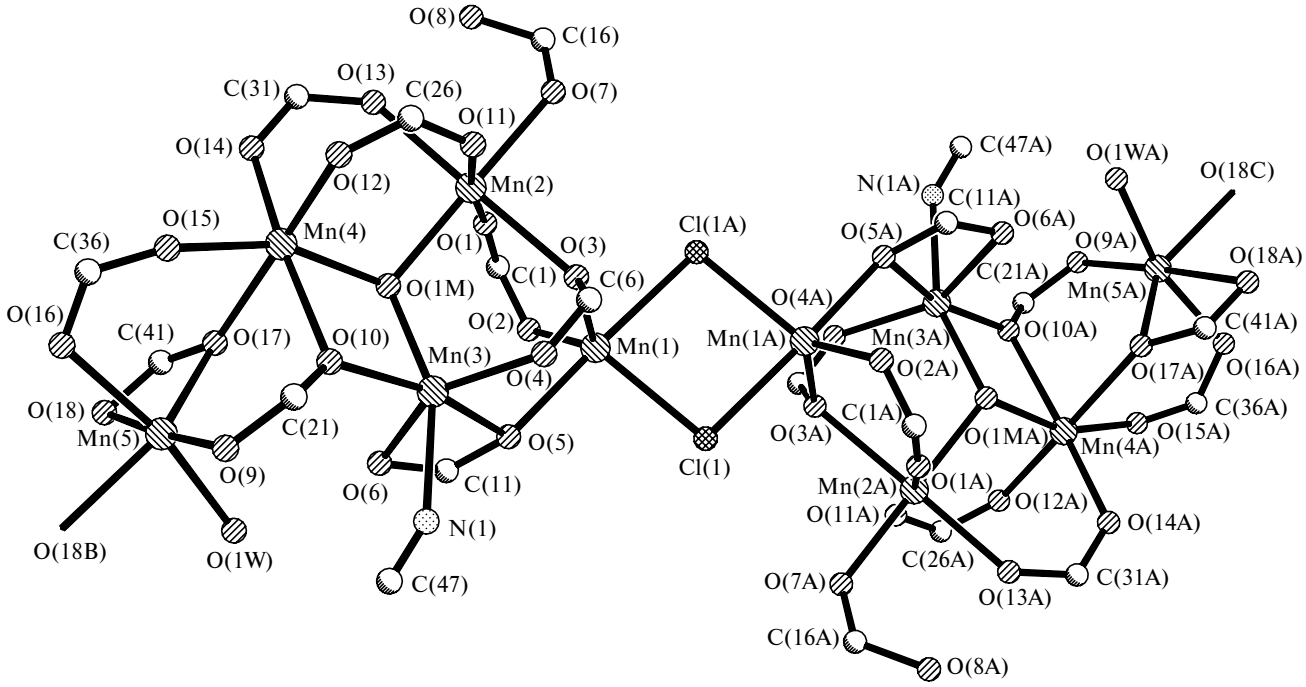

Fig. 2. Fragment of the polymer chain of **4** (*tert*-butyl substituents at the carboxylate groups are omitted).

Two additional manganese atoms are bound to the metal atoms of the triangle (Mn...Mn, 3.542(3)—3.607(3) Å). One of these atoms is coordinated to two chlorine atoms serving as bridges between the pentanuclear fragments of the metal chain (Mn—Cl, 2.427(4) and 2.581(4) Å) and three oxygen atoms of the bridging pivalate groups having different dentation (Mn—O, 2.056(10), 2.131(8), and 2.209(9) Å). Another peripheral manganese atom is linked to the triangle by two bridging carboxylate groups (Mn—O, 2.085(9)—2.142(9) Å) and is coordinated by the water molecule (Mn—O, 2.223(10) Å) and the chelating carboxylate group (Mn—O, 2.263(7) and 2.356(9) Å). The latter, in turn, also serves as a bridge between the adjacent pentanuclear fragments of the metal chain (Mn—O, 2.114(9) Å). The magnetic properties of coordination compound **4** are analogous to those of polymeric pivalate **1** studied earlier. A decrease in the temperature to 2 K leads to a decrease in μ_{eff} of complex **4** to 3.29 μ_B (Fig. 3), which is evidence for the dominating antiferromagnetic interactions in this compounds. The efficiency of interactions is rather high because μ_{eff} is 12.57 μ_B already at 300 K. This value is similar to the pure-spin value of 13.2 μ_B for five weakly interacting Mn^{II} ions with the spin S = 5/2. In the temperature range of 100—300 K, the magnetic susceptibility follows the Curie—Weiss law with the following parameters: C = 23.2±0.2 K cm^3 mol^{-1}, θ = −52.3±0.2 K.

Formally, polymers **1** and **4** are similar in the magnetic properties, which makes it difficult to estimate the purity of the starting compounds used in further syntheses by magnetic methods. However, pure polymer **1** (purity was confirmed by elemental analysis for chlorine and spectroscopic characteristics) can be prepared by this reaction with the use of the pivalate anion : manganese atom ratio of 2 : 1.

The reaction of polymer **1** with an excess of pivalic acid in hexane or acetonitrile (t > 68 °C) leads to removal of the coordinated ethanol molecules giving rise to virtually the only product, *viz.*, the $[Mn_4(OOCBu^t)_8(HOOCBu^t)_2]_n$ polymer (**5**) (Scheme 2). The structure of compound **5** was established by X-ray diffraction[4] (Table 1).

The magnetic behavior of polymer **5** is qualitatively analogous to the above-described behavior of complex **4** (see Fig. 3). The magnetic moment μ_{eff} decreases from 11.19 to 2.13 μ_B in the temperature range of 300—2 K due to antiferromagnetic exchange interactions. At high temperatures, the curve $1/\chi(T)$ for **5** is described by the Curie—Weiss equation with the following parameters: C = 17.4±0.1 K cm^3 mol^{-1}, θ = −33.3±0.3 K.

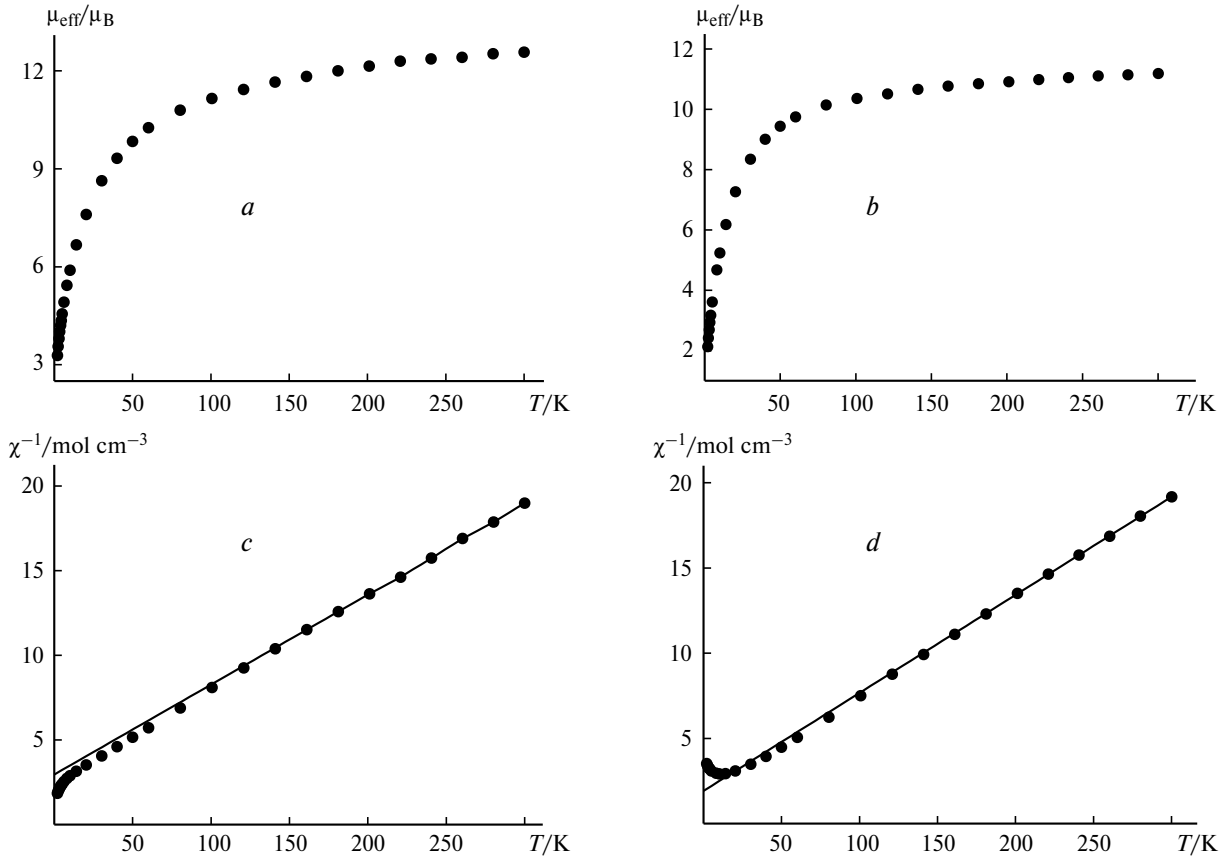

Fig. 3. Plots of $\mu_{eff}(T)$ (*a*, *b*) and $1/\chi(T)$ (*c*, *d*) for polymers **4** (*a*, *c*) and **5** (*b*, *d*).

Scheme 2

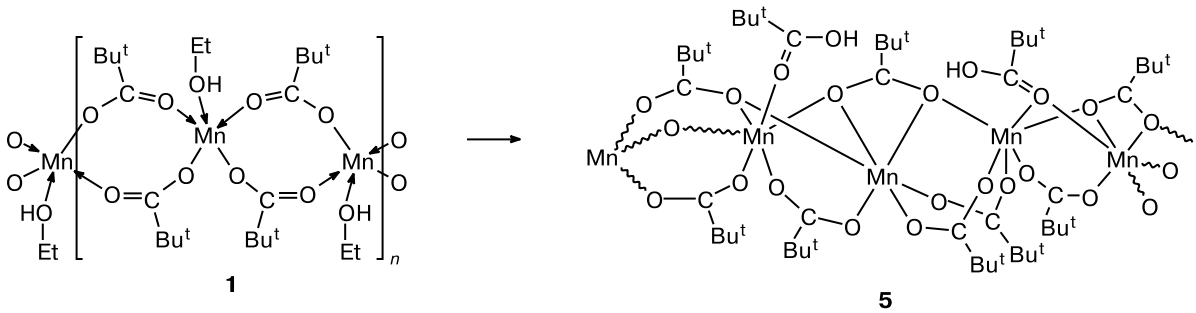

1 **5**

Reagents and conditions: $HOOCBu^t$, MeCN, or hexane, Ar.

Unlike the reaction of the manganese-containing pivalate polymer, the analogous reaction of polymeric iron(II) pivalate $[Fe(\mu\text{-}OOCBu^t)_2]_n$ (**3**) with pivalic acid in hexane (68 °C, [Fe] : $HOOCBu^t$ = 1 : 4) affords the mononuclear compound $Fe(\eta^1\text{-}OOCBu^t)_2(\eta^1\text{-}HOOCBu^t)_4$ (**6**) (Scheme 3).

Complex **6** can also be prepared starting from the tetranuclear complex $Fe_4(\mu_3\text{-}OH)_2(\mu\text{-}OOCBu^t)_4(\eta^2\text{-}OOCBu^t)_2(\eta^1\text{-}EtOH)_6$ (**7**)[7] (hexane, 68 °C, [Fe] : $HOOCBu^t$ = 1 : 5) (see Scheme 3).

X-ray diffraction study demonstrated that the metal atom in mononuclear complex **6** is coordinated by six oxygen atoms of two pivalate groups and four pivalic acid molecules (Fe—O, 2.075(2)—2.166(2) Å; C—O(OOCR), 1.242(4)—1.277(4) Å; C—O(HOOCR), 1.214(4)—1.314(4) Å) (Fig. 4). The hydrogen atoms of the hydroxy fragments of coordinated carboxylic acids are involved in intramolecular hydrogen bonding with the terminal (O—H...O, 1.69 Å) or coordinated (O—H...O 1.79—1.80 Å) oxygen atoms of the pivalate anions (see Fig. 4).

The magnetic moment μ_{eff} of mononuclear complex **6** changes weakly in the temperature range of 300—40 K (5.14—4.93 μ_B) (Fig. 5). At room temperature, the magnetic moment μ_{eff} is characteristic of the high spin Fe^{II} ion. Only after a decrease in the temperature to 2 K, μ_{eff} monotonically decreases to 3.38 μ_B due to the appearance of weak intermolecular antiferromagnetic interactions.

The tendency of Mn^{II} pivalate **1** to retain the polymer structure in spite of an excess of pivalic acid in the reaction system is an important difference in the chemical

Table 1. Crystallographic parameters for complexes **4—6** and **11—13**

Parameter	**4**	**5**	**6**	**11**	**12**	**13**
Molecular formula	$C_{49}H_{90}ClMn_5N_2O_{20}$	$C_{50}H_{90}Mn_4O_{20}$	$C_{30}H_{58}FeO_{12}$	$C_{23}H_{38}Fe_{1.5}N_3O_6$	$C_{34}H_{50}FeN_8O_4$	$C_{34}H_{54}FeN_6O_4$
Space group	$P2_1/n$	$P\bar{1}$	$P2_1/c$	$C2/c$	$P2_1/c$	$P\bar{1}$
a/Å	14.653(7)	11.7317(7)	17.308(5)	21.594(6)	8.894(2)	12.932(6)
b/Å	21.236(11)	12.4788(7)	10.579(3)	11.131(3)	17.931(5)	16.430(8)
c/Å	21.130(11)	22.0506(13)	21.370(7)	22.158(5)	22.772(5)	19.325(8)
α/deg	90	92.6120(10)	90	90	90	77.479(7)
β/deg	91.639(18)	95.7350(10)	105.571(9)	92.743(7)	99.455(6)	73.210(13)
γ/deg	90	98.7340(10)	90	90	90	70.719(9)
V/Å^3	6572(6)	3168.7(3)	3769(2)	5320(2)	3582.2(14)	3677(3)
Z	4	2	4	8	4	4
ρ_{calc}/g cm^{-3}	1.352	1.290	1.175	1.339	1.281	1.204
μ/cm^{-1}	10.40	8.43	4.52	8.69	4.69	4.53
Number of measured reflections	22995	19606	21823	10067	21517	24425
Number of reflections with $I > 4.0\sigma$	9928	14311	7846	4559	8175	15273
R_1	0.0894	0.0526	0.0744	0.0692	0.0794	0.0593
wR_2	0.1673	0.1308	0.1894	0.1501	0.1956	0.1482

Scheme 3

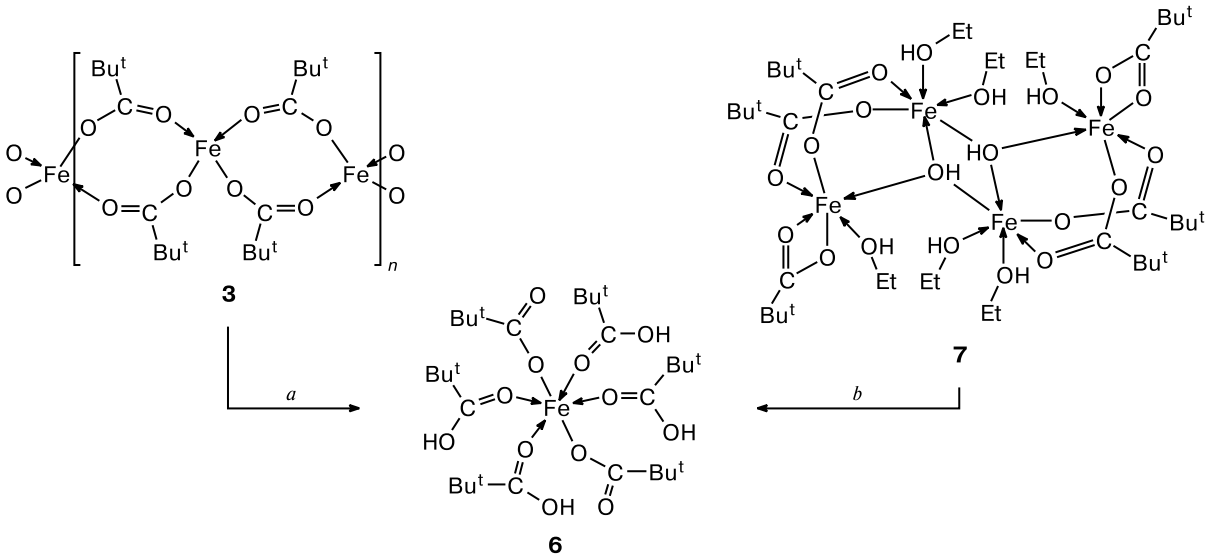

Reagents and conditions: *a*. HOOCBu^t ([Fe] : L = 1 : 4), hexane, 68 °C, Ar; *b*. HOOCBu^t ([Fe] : L = 1 : 5), hexane, 68 °C, Ar.

properties of the manganese and iron polymers. Unlike compound **1**, iron(II) polymer **3** is readily decomposed in the presence of the excess acid to give high spin mononuclear complex **6** containing 18-electron octahedral Fe^{II} ions in spite of the formal electron deficiency (14-electron iron atoms are in a tetrahedral environment) and coordination deficiency of the metal centers. Apparently, this signifies that the strength of binding of the metal atoms with the bridging pivalate groups in the manganese polymers differs from that in the iron polymers in spite of the relative similarity of the structural fragments of these polymers, which are chains consisting of the metal atoms linked to each other by pairs of pivalate bridges (Fig. 6).

To qualitatively estimate the stability of the starting polymers, we studied thermolysis of these compounds in the solid state. We found that decomposition of polymeric manganese pivalate **1** starts already at 60 °C. In the temperature range of 60—100 °C, the weight loss of 14.5±1.5% is observed (which corresponds to removal of the coordinated ethanol molecule and the possible formation of the $[Mn(\mu\text{-}OOCBu^t)_2]_n$ compound, whose composition is analogous to that of iron polymer **3**). This process is accompanied by energy consumption (endothermic effect with a shoulder) (Fig. 7). In the temperature range of 100—205 °C, the weight remains unchanged, but energy absorption is observed, which apparently corresponds to the structural rearrangement of the new polymer. At temperatures above 205 °C, the weight loss and melting of the

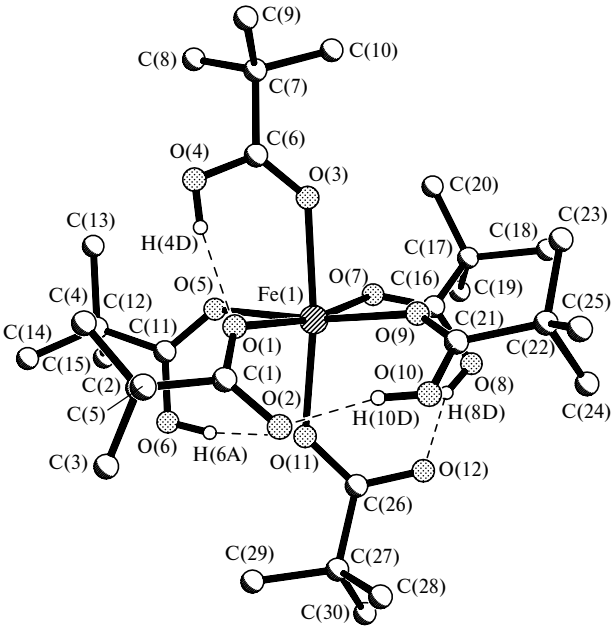

Fig. 4. Structure of complex **6**.

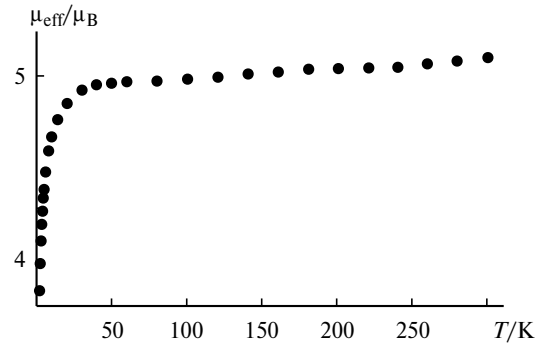

Fig. 5. Plot of $\mu_{eff}(T)$ for mononuclear complex **6**.

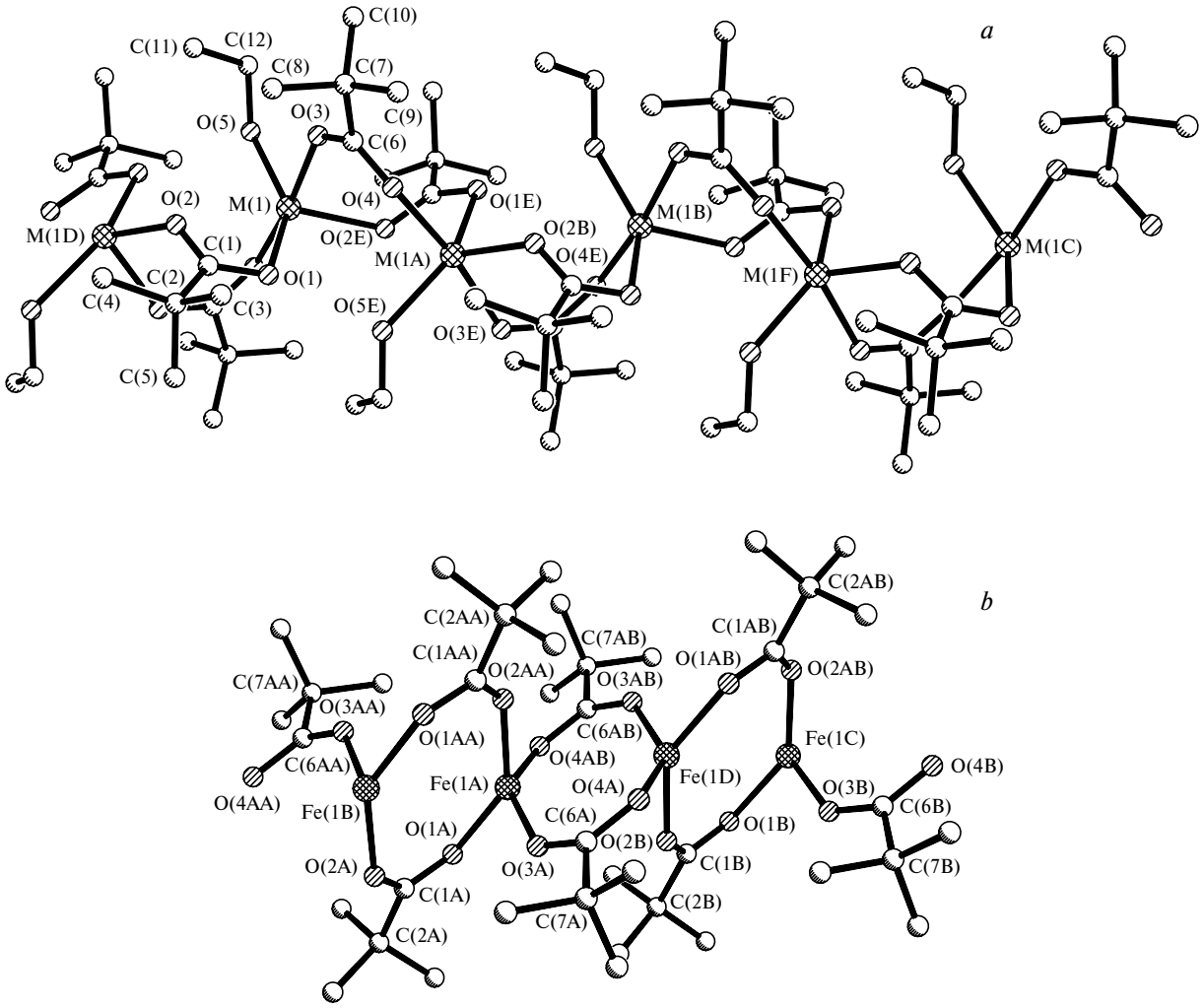

Fig. 6. Structures of polymers **1** (M = Mn, see Ref. 6), **2** (M = Fe, see Ref. 7) (*a*), and **3** (see Ref. 7) (*b*).

intermediate occur. The melting point is 214.5±3.0 °C. The weight loss ceases at 400 °C. Processes accompanied by energy release start almost simultaneously with the cessation of weight loss. The total weight loss is 75±1.5%. The weight of the solid product is 25±1.5%. Mixed-valent oxide Mn_3O_4 was obtained as the final decomposition product (Table 2).

As opposed to manganese polymer **1**, the initial step of heating of iron-containing polymer **3** is accompanied by energy changes without changes in the weight. In the temperature range of 100—220 °C, energy release is observed due, apparently, to polymer destruction and the formation of intermediate polynuclear structures. At temperatures above 203 °C, changes accompanied by the weight loss start. The melting point is 230.0±3.0 °C. Presumably, this value corresponds to a new compound, *viz.*, a decomposition product of the polymer, because the weight loss is as large as 9.5±1.5% when melting begins. This value approximately corresponds to the loss of one pivalate anion from four $Fe(\mu\text{-}OOCBu^t)_2$ units (see Fig. 7). On the background of complex energy changes, a further decrease in the weight is observed, and the weight loss is 60.5±1.5%. The total weight loss is 70±1.5%. The weight of the solid residue is 30.0±1.5%. Iron(III) oxide $\gamma\text{-}Fe_2O_3$ was obtained as the final decomposition product (see Table 2).

The $[Fe(\mu\text{-}OOCBu^t)_2(\eta\text{-}EtOH)]_n$ polymer (**2**) is isostructural to polymer **1**. Thermolysis of **2** could be expected to combine the characteristic features of thermal decomposition typical of both polymers **1** and **3**. However, even the initial step of heating of **2** occurs differently, which is reflected in the shape of the first endothermic peak, where a pronounced shoulder is observed in the temperature range of 40—80 °C. Apparently, this effect is associated with the crystal rearrangement (see Fig. 7). Decomposition of **2** starts at a temperature higher than 60 °C. The initial process is accompanied by a considerable endothermic effect, and the weight loss is 15.1±1.5% (this step corresponds to removal of coordinated ethanol). Presumably, removal of ethanol gives rise

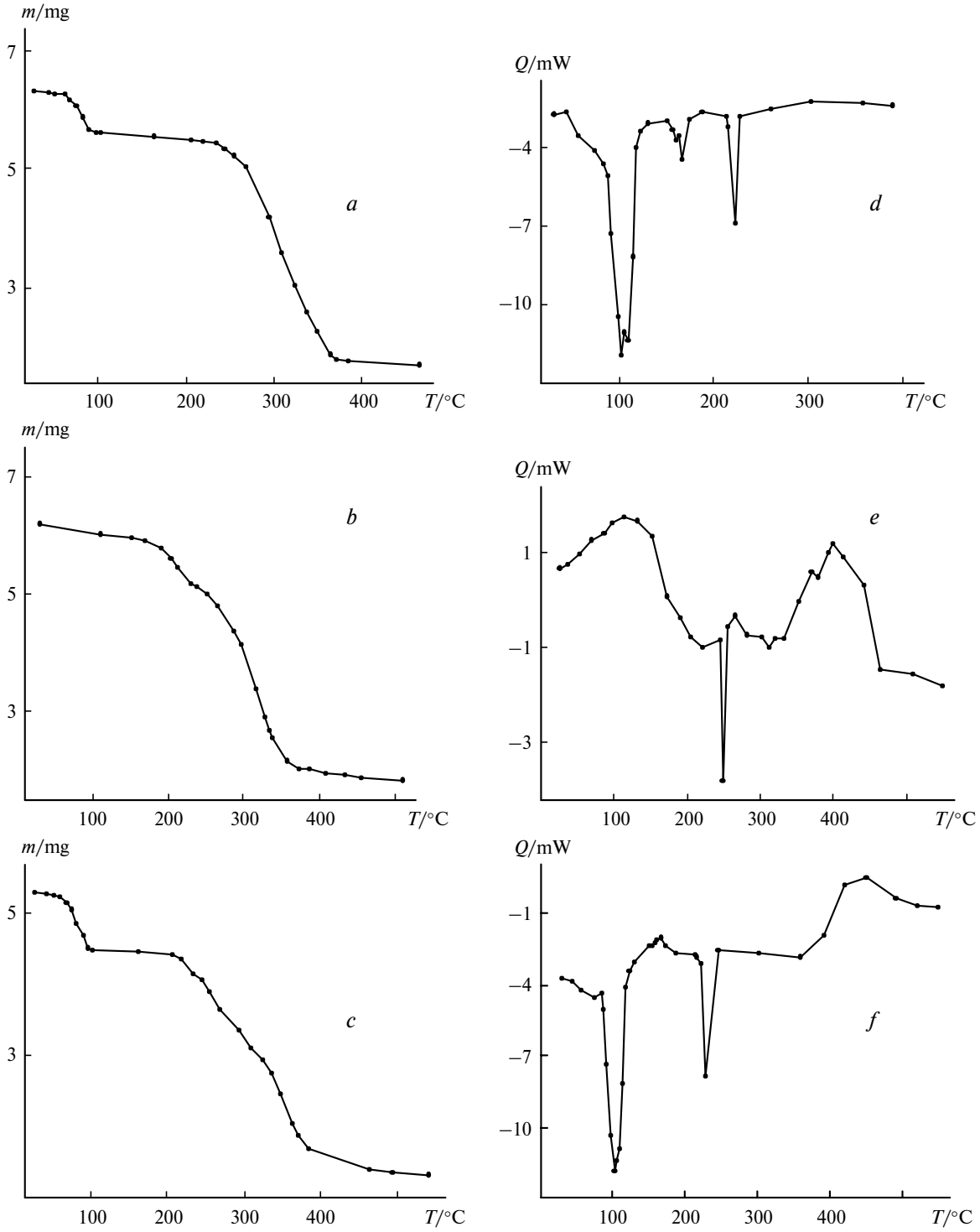

Fig. 7. Plots of the thermal flow *vs.* the temperature for polymers **1** (*a*), **3** (*b*), and **2** (*c*) and the integral dependence of the change in the weight of polymers **1** (*d*), **3** (*e*), and **2** (*f*) during heating.

to a product analogous to polymer **3**. The identity of **3** to the product of decomposition of polymer **2** to 100 °C was confirmed by calorimety (Table 3 and Fig. 8). In the temperature range of 110—200 °C, the weight of the thermolyzed intermediate, like that of polymer **3**, remains virtually unchanged, but energy release is observed (blurred exothermic effect). At temperatures above 206 °C, the weight loss starts. As in the case of **3**, when melting of **2** begins (melting point is 222.0±5.0 °C), the weight loss is 8.0±2.0%. At temperatures above 390 °C, the exo-

Table 2. X-ray powder diffraction analysis of decomposition products of polymer complexes **1—3**

Decomposition product of **1**		Decomposition product of **2**		Decomposition product of **3**		Mn_3O_4*		γ-Fe_2O_3**	
d/Å	*I* (%)	*d*/Å	*I* (%)	*d*/Å	*I* (%)	*d*/Å	*I* (%)	*d*/Å	*I* (%)
4.950	40					4.924	30		
3.090	60					3.089	40		
		2.945	30	2.950	40			2.950	30
2.870	10					2.881	17		
2.768	50					2.768	85		
		2.522	100	2.520	100			2.514	100
2.490	100					2.487	100		
2.360	10					2.367	20		
		2.090	10	2.092	10			2.086	15
2.045	30					2.037	20		
						1.830	10		
1.790	20					1.799	25		
1.705	20					1.700	20		
		1.605	20	1.605	20			1.604	20
1.575	20					1.576	25		
1.541	50					1.544	50		
		1.465	30	1.475	20			1.474	40
1.430	20					1.440	30		

* *Powder Diffraction File*, Swarthmore: Joint Committee on Powder Diffraction Standards, card no. 24-734.
** *Powder Diffraction File*, Swarthmore: Joint Committee on Powder Diffraction Standards, card no. 25-1402.

Table 3. Temperature dependence of the heat capacity for $[Fe(OOCBu^t)_2]_n$ (**1**), the polymer $[Fe(\mu\text{-}OOCBu^t)_2(EtOH)]_n$ (**2**), and the product of decomposition of **2** to 100 °C

T/K	$C_p \pm 2$/J K^{-1} mol^{-1}		
	3	Decomposition product of **2**	**2**
143	243.4	243.1	294.2
153	254.9	254.4	315.1
163	266.7	267.0	325.4
173	276.4	275.3	340.2
183	285.9	285.1	351.6
193	297.4	296,5	362.3
203	307.5	306,2	374.8
213	317.7	316.4	386.4
223	328.5	327,8	400.9
233	339.3	338.3	409.5
243	348.8	348.9	420.8
253	359.5	360.5	432.0
263	369.6	369.2	444.0
273	378.6	378.6	456.1
283	389.2	389.0	464.8
293	395.4	395.7	476.5
303	405.0	404.1	487.7

thermic effect is observed. Decomposition is completed at 490 °C. The total weight loss is 74.0±2.0%. The weight of the solid product is 26.0±2.0%. Decomposition of polymer **1**, like that of polymer **3**, affords γ-Fe_2O_3 (see Table 2).

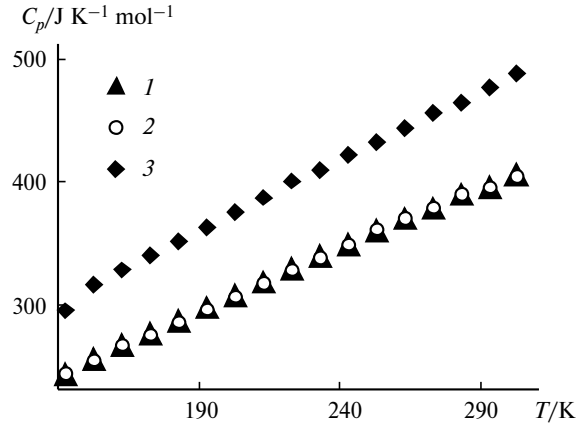

Fig. 8. Plots of the heat capacity *vs.* the temperature for compound **3** (*1*), the decomposition product of **2** (*2*), and compound **2** (*3*).

Study of solid-state thermolysis of the pivalate polymers unambiguously revealed a stable species existing in the temperature range of 60—100 °C. Although the behavior of this phase of the manganese derivatives described by the formula $[M(OOCBu^t)_2]_n$ differs from that of the analogous iron derivatives, it is apparently this phase that is most active in chemical reactions. In addition, it is evident that decomposition of the stable phase at >200 °C is accompanied by intramolecular oxidation of the metal atoms because, in spite of the inert conditions (thermolysis was studied under argon), decomposition of the

Mn^{II}- and Fe^{II}-containing polymers affords oxides containing Mn^{III} and Fe^{III} ions.

Unlike the carboxylate anion, which generally forms OCO bridges, *o*-phenylenediamine molecules contain two donor nitrogen atoms separated by two carbon atoms of the phenylene ring (NCCN fragment). Examples, where such molecules form a four-atom bridge between VII and VIII Group 3d transition metals, have been documented[11] although these molecules generally readily form stable five-membered metallocycles.[11–13] The latter can be oxidized to give metal semiquinonediimine fragments[14–17] or even diimine complexes.[14,18] Earlier,[7] we have demonstrated that the reaction of polymer **1** with a deficiency of 1,2-$(NH_2)_2(C_6H_2R_2)$ (R = H or Me) ([Mn] : L ≥ 3 : 2) produces the antiferromagnetic [2+1] polymers $\{[(\eta^2\text{-}(NH_2)_2C_6H_2R_2)_2Mn(\mu\text{-}OOCBu^t)_2][Mn_2(\mu\text{-}OOCBu^t)_4]\}_n$ (**8** and **9**) (R = H (**8**) or Me (**9**)) containing alternating di- and mononuclear fragments. Among these compounds, only the latter contain the chelating *o*-phenylenediamine ligands. The iron-containing analog $\{[(\eta^2\text{-}(NH_2)_2C_6H_2R_2)_2Fe(\mu\text{-}OOCBu^t)_2][Fe_2(\mu\text{-}OOCBu^t)_4]\}_n$ (**10**) (R = Me) exhibiting the ferrimagnetic properties was synthesized analogously from polymer **2** and 1,2-$(NH_2)_2(C_6H_2Me_2)$. However, we failed to synthesize the polymer with R = H according to this method.

In the present study, we used polymer **3** in which coordinated ethanol molecules are absent as the starting iron-containing reagent. It appeared that the reaction of **3** with 1,2-$(NH_2)_2(C_6H_4)$ (MeCN, 80 °C, [Fe] : L = 3 : 2) produces the $\{[(\eta^2\text{-}(NH_2)_2C_6H_4)_2Fe(\mu\text{-}OOCBu^t)_2][Fe_2(\mu\text{-}OOCBu^t)_4]\cdot 2MeCN\}_n$ polymer (**11**·2MeCN) in high yield (Scheme 4).

X-ray diffraction study demonstrated that polymer **11**, like its manganese-containing analog **8**, as well as derivatives **9** and **10** with methyl-substituted *o*-phenylenediamine ligands, consist of alternating di- and mononuclear fragments (Fig. 9). In the dinuclear fragment of compound **11**, the metal atoms are linked together by four bridging carboxylate groups (Fe...Fe, 2.880(2) Å; Fe—O, 2.073(4) Å). The mononuclear fragment of the chain consists of the metal atom coordinated by two chelating 1,2-phenylenediamine molecules and two pivalate groups in *trans* positions with respect to each other, which link the mononuclear and two dinuclear fragments (Fe...Fe, 4.533(2) Å; Fe—Fe—Fe, 144.4°; Fe—N, 2.241(5) Å; Fe—O, 2.036(4) Å).

The plot of $\mu_{eff}(T)$ for complex **10** substantially differs from that for complex **11** (Fig. 10). At near room temperature, μ_{eff} of complex **11** is 8.98 μ_B, which is near the theoretical limit (8.48 μ_B) for three weakly interacting

Scheme 4

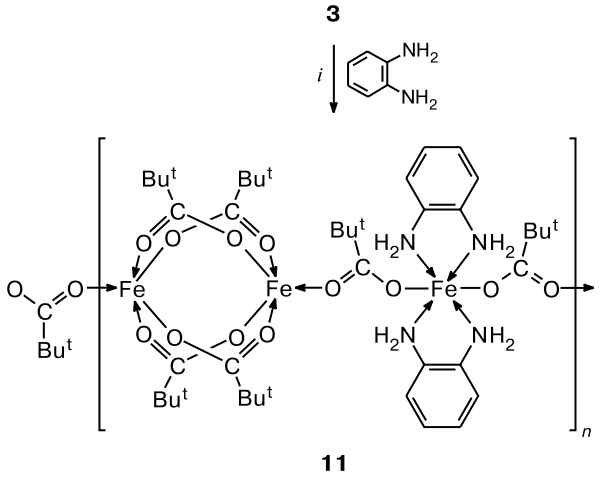

i. MeCN, 80 °C, Ar.

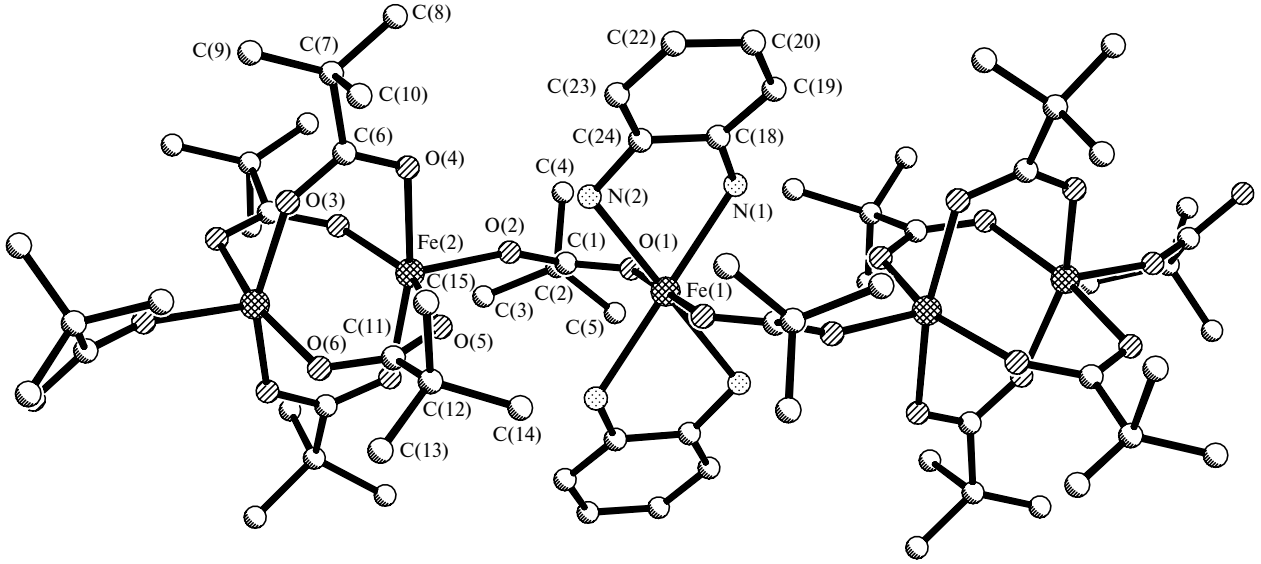

Fig. 9. Fragment of the polymer chain of complex **11**.

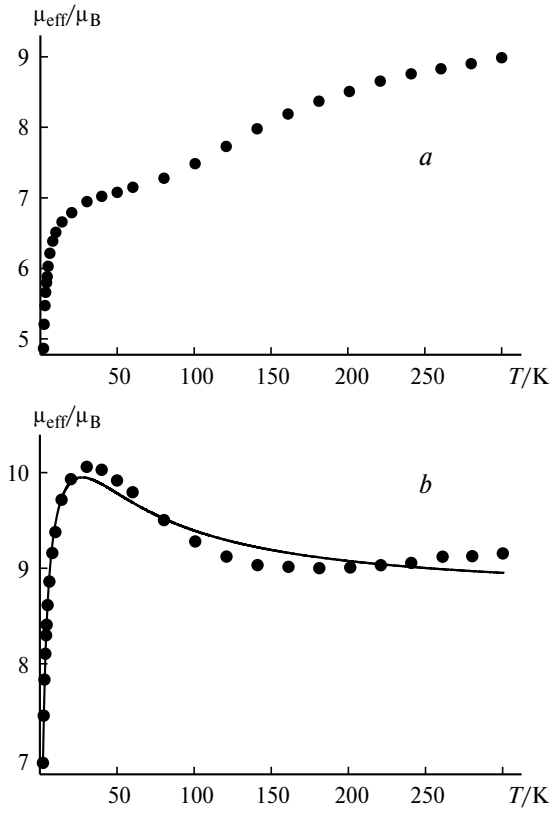

Fig. 10. Plots pf $\mu_{eff}(T)$ for iron-containing polymers **11** (*a*) and **10** (*b*) (theoretical data are shown by a solid curve).

spins S = 2 with the *g* factor of 2. The magnetic moment μ_{eff} tends to saturation at ~7.1 μ_B with decreasing temperature. At <20 K, the curve $\mu_{eff}(T)$ falls off sharply and reaches 4.87 μ_B at 2 K. The plot of $\mu_{eff}(T)$ for complex **11** formally represents two types of antiferromagnetic exchange interactions different in value. It should be noted that in the temperature range from 300 K to 50 K, strong antiferromagnetic exchange interactions in the four-bridge dimeric fragments make the largest contribution to the magnetic behavior of **11**, whereas weaker antiferromagnetic interactions between the dimers and monomers involving various weak interchain exchange interactions are efficiently included at temperatures near 20 K. The latter interactions lead to a substantial decrease in μ_{eff} at helium temperatures. However, the magnetic behavior of compound **11** is unusual in that the magnetic moment μ_{eff} is virtually constant in the temperature range of 30—100 K, and this value is near the theoretical limit of 6.92 μ_B for two noninteracting spins S = 2 with the *g* factor of 2. In our opinion, this magnetic behavior of compound **11** can be attributed to two factors. First, this can be associated with the fact that a decrease in the temperatures leads to the appearance of the ferromagnetic contribution to exchange interactions between the Fe^{II} ions due, for example, to structural changes in the crystal. The observed magnetic behavior can also be accounted for by the transition of the Fe^{II} ions in the mononuclear fragments of the polymer chain of **11** to the low-spin state (S = 0). In spite of the good quantitative description, the possibility of the spin transition in complex **11** is somewhat doubtful because an analogous effect has been early observed only for Fe^{II} coordination compounds in which the Fe^{II} ions are coordinated by six nitrogen atoms, whereas there are only four nitrogen atoms in the complex in question. Therefore, a decrease in μ_{eff} of **11** in the temperature range of 100—200 K is most likely caused by a phase transformation rather than exclusively by antiferromagnetic exchange interactions.

For polymer **10** (R = Me), the magnetic moment μ_{eff} gradually decreases in the temperature range of 300—140 K from 9.16 to 9.03 μ_B (see Fig. 10, *b*). The magnetic moment μ_{eff} increases to 10.06 μ_B as the temperature decreases to 30 K, which indicates that ferromagnetic exchange interactions dominate in the crystal of **10**. Then μ_{eff} decreases to 6.96 μ_B at 2 K due to the appearance of intermolecular antiferromagnetic interactions. We estimated exchange interactions in the repeating Fe(1)...Fe(2)...Fe(3) fragment. Calculations for this cluster in terms of the isotropic Hamiltonian were carried out with the use of the program described in the study.[19] Let us denote the exchange interaction parameter in the dimer by J_{12} and the corresponding parameter between the dimer and monomer by J_{23}. Then the optimization gave the following Hamiltonian parameters: $g_1 = g_2 = 2.09(2)$, $g_3 = 2.00(2)$, $J_{12} = 5.27(9)$ cm^{-1}, and $J_{23} = -0.18(7)$ cm^{-1}, and the intermolecular exchange parameter $nJ' = -0.06(2)$ cm^{-1}. Earlier,[20] the ferromagnetic character of exchange interactions was assumed for the four-bridge Fe^{II} dimers $L_2Fe_2(\mu\text{-}OOCR)_4$ (HOOCR is 2,6-di(*p*-tolyl)benzoic acid and L is benzylamine or methoxybenzylamine). Recently,[10] the strong ferromagnetic contribution to exchange interactions in the dinuclear complex $(2,3\text{-}Me_2C_5H_3N)_2Fe_2(\mu\text{-}OOCBu^t)_4$ has been explained based on calculations taking into account the orbital component.

As expected, an excess of the *o*-phenylenediamine ligands in the reaction mixture leads to the formation of mononuclear complexes. For example, the reaction with an excess of 1,2-phenylenediamine ([Fe] : L = 1 : 4) or 4,5-dimethyl-1,2-phenylenediamine ([Fe] : L = 1 : 3) with the tetranuclear complex $Fe_4(\mu_3\text{-}OH)_2(\mu\text{-}OOCBu^t)_4(\eta^2\text{-}OOCBu^t)_2(\eta^1\text{-}EtOH)_6$ (**7**) (or polymer **3**) in ethanol at 80 °C produces the $Fe(\eta^1\text{-}OOCBu^t)_2(\eta^1\text{-}(NH_2)_2C_6H_4)_4$ (**12**) and $Fe(\eta^1\text{-}OOCBu^t)_2(\eta^2\text{-}(NH_2)_2C_6H_2Me_2)(\eta^1\text{-}(NH_2)_2C_6H_2Me_2)_2$ (**13**) complexes, respectively, in good yields (40% for **12** and 61% for **13**) (Scheme 5).

X-ray diffraction study (Fig. 11) demonstrated that the iron atom in complex **12** is in a distorted octahedral coordination environment formed by four nitrogen atoms of the amino groups of four diamine ligands in the equa-

Scheme 5

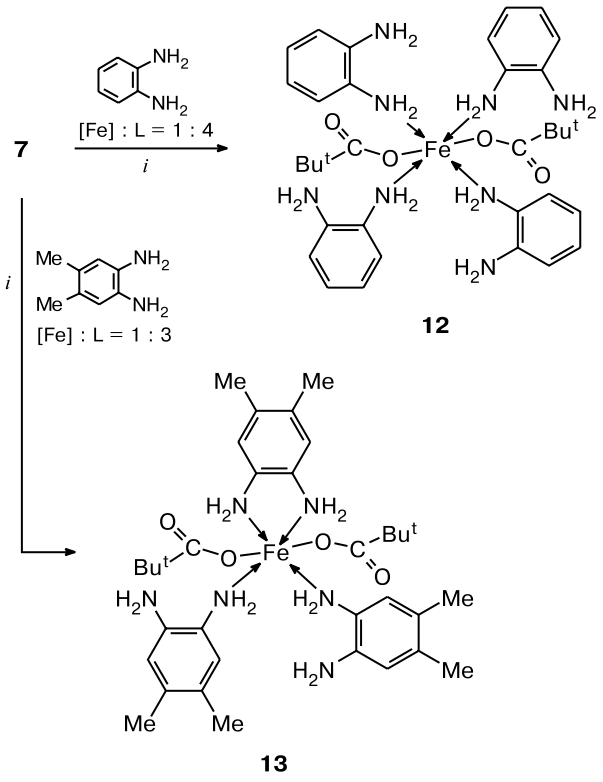

i. EtOH, 80 °C, Ar.

torial plane (Fe—N, 2.256(2)—2.322(2) Å; N—Fe—N, 86.83(7)—93.51(7)°) and two oxygen atoms of the carboxylate groups in the axial positions (Fe—O, 2.0344(18) and 2.0425(18) Å; O—Fe—O, 179.31(7)°). In the crystal, the molecules of the mononuclear complex are linked to each other by hydrogen bonds between the protons of the free amino groups of the diamine ligands and the oxygen atoms of the terminal pivalate groups ($N(NH_2)$...O(OOCR), 2.844 and 2.885 Å) to form a supramolecular network (see Fig. 11). In addition, there are stacking interactions between the phenylene rings of the *o*-phenylenediamine ligands of the adjacent molecules (distances between the planes of the rings are in the range of 3.424—3.490 Å).

Complex **13**, unlike mononuclear complex **12**, contains only three diamine ligands, one of them being coordinated in a chelate fashion (Fig. 12). The equatorial plane in complex **13**, like that in **12**, is formed by four nitrogen atoms of four amino groups (Fe—N, 2.204(2)—2.258(2) Å; N—Fe—N(η^2-L), 74.61(8)° and 74.57(4)°; N—Fe—N, 92.28(8)—97.42(8)° and 92.59(8)—96.39(8)° in two independent molecules). Two oxygen atoms of the pivalate ligands are in the axial positions (Fe—O, 2.081(2)—2.0931(18) Å; O—Fe—O, 172.27(7)°, 170.64(8)°). The molecules of the mononuclear complex in the crystal structure of **13** are also linked to each other by hydrogen bonds ($N(NH_2)$...O(OOCR), 2.814—2.989 Å) and stacking in-

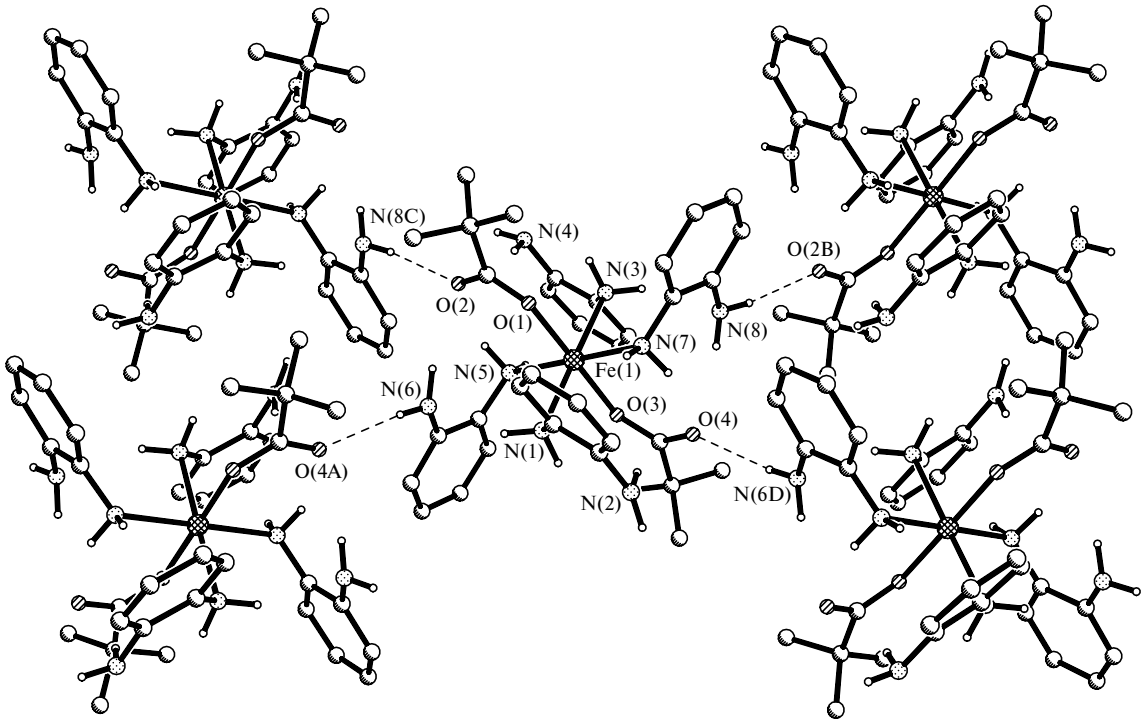

Fig. 11. Fragment of the crystal packing of mononuclear complex **12**.

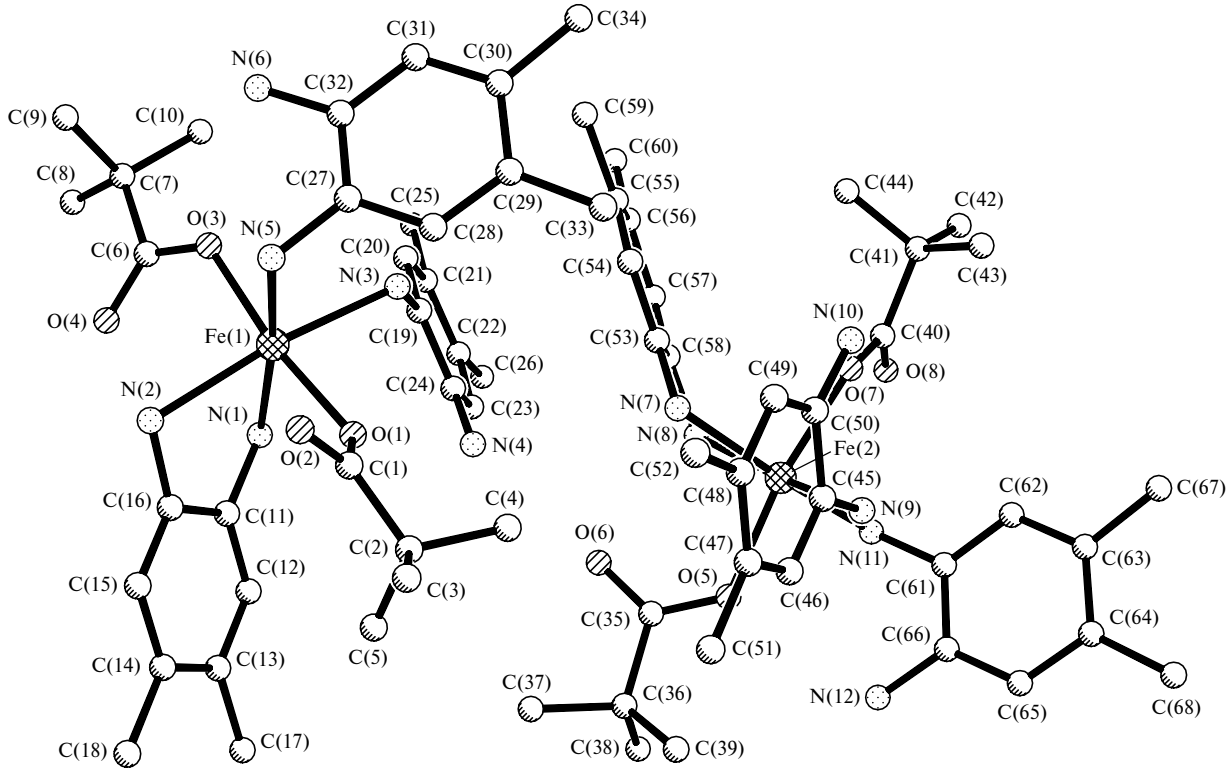

Fig. 12. Structure of complex **13** (two crystallographically independent geometrically similar molecules are shown).

teractions (distances between the planes of the phenylene fragments in the adjacent molecules are in the range of 3.367—3.623 Å) to form a supramolecular network (see Fig. 12).

The magnetic behavior of **12** and **13** is similar to that of mononuclear complex **6**. The effective magnetic moments of **12** and **13** are very weakly temperature-dependent in the range of 300—20 K (5.00—4.93 μ_B for **12** and 5.00—4.96 μ_B for **13**) (Fig. 13). Only at helium temperatures, μ_{eff} monotonically decreases (4.66 μ_B (4.2 K) for **12** and 4.12 μ_B (2 K) for **13**) due to the appearance of weak intermolecular antiferromagnetic exchange interactions.

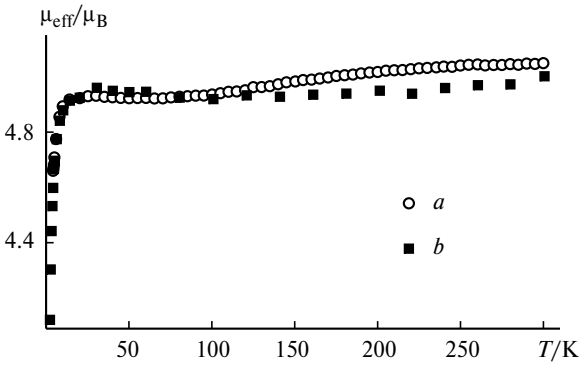

Fig. 13. Plots of $\mu_{eff}(T)$ for mononuclear complexes **12** (*a*) and **13** (*b*).

As a result, the reaction with an excess of *o*-phenylenediamines, like the reactions of the iron polymer with pivalic acid, leads to degradation of the polymeric structure and the formation of mononuclear complexes.

The polymeric Mn^{II} and Fe^{II} pivalates under study are suitable for use as the starting "spin materials" from which magnetic molecules with a desired geometry can be generated. In this case, information on the tendency of the manganese derivative to retain a polynuclear (even polymeric) structure in the presence of excess carboxylic acid or *o*-phenylenediamine is undoubtedly useful in the development of procedures for the formation of nanosized molecular magnets containing high spin Mn^{II} atoms. The possibility to generate carboxylate or diamine monomers with Fe^{II} atoms, which are readily soluble in hydrocarbons, holds promise that new procedures will be developed for the formation of heteronuclear magnetic structures assembled from such monomers and coordinatively unsaturated magnetoactive polymers analogous to compound **1**. All polymeric Mn^{II} pivalates have the antiferromagnetic properties in spite of substantial structural differences. At the same time, analogous Fe^{II} derivatives exhibit the ferromagnetic properties. This fact is important for the choice of the starting "spin material" and, apparently, should be taken into account when designing the process of assembly of new molecular magnets.

Experimental

The complexes were synthesized under pure argon with the use of freshly distilled solvents. The starting $[Mn(OOCBu^t)_2(HOEt)]_n$ (**1**),[6] $[Fe(OOCBu^t)_2]_n$ (**3**),[7] and $[Fe_4(\mu_3\text{-}OH)_2(\mu\text{-}OOCBu^t)_4(\eta^2\text{-}OOCBu^t)_2(\eta^1\text{-}EtOH)_6]\cdot 2EtOH$ (**7**·2EtOH)[7] compounds were synthesized according to known procedures. Commercial $MnCl_2\cdot 4H_2O$ (special purity), KOH (chemical purity), pivalic acid, 4,5-dimethyl-1,2-phenylenediamine, and 1,2-phenylenediamine (Fluka) were used in the synthesis of new compounds.

The IR spectra were recorded on a Specord M-80 instrument in KBr pellets. The magnetochemical measurements were performed at the International Tomography Center of the Siberian Branch of the Russian Academy of Sciences (Novosibirsk) on a SQUID magnetometer (MPMS-5S Quantum Design) in the temperature range of 2—300 K using the magnetic field intensity of up to 5 kOe. The molar magnetic susceptibility (χ) was calculated taking into account the atomic diamagnetism according to the additive Pascal scheme. In the paramagnetic region, the effective magnetic moment was calculated by the equation $\mu_{eff} = [(3k/N_A\beta^2)\chi T]^{1/2} \approx (8\chi T)^{1/2}$,[21] where k is the Boltzmann constant, N_A is Avogadro's number, and β is the Bohr magneton.

Thermal decomposition of compounds **1—3** was studied by differential scanning calorimetry and thermogravimetry on DSC-20 and TG-50 units of a TA-3000 thermoanalyzer (Mettler). Samples were heated under dry argon at a constant rate (in all experiments) of 5 deg min^{-1}. For each compounds, four differential scanning calorimetry experiments and three thermogravimetry experiments were performed. The weight loss upon thermal destruction was determined directly on a TG-50 thermobalance; the accuracy of weighing was $\pm 2\cdot 10^{-3}$ mg. Stepwise thermal decomposition was studied by differential scanning calorimetry, which involved the division of the total temperature range into parts. The size and number of these parts were determined based on the overall pattern of the weight and energy changes upon decomposition. This approach allowed us to determine the weight loss in each temperature range and compare the results of DSC with the thermogravimetric data. The results of these methods were in satisfactory agreement, which confirms the reliability of the experimental data. The accuracy of the determination of the anomalous points and thermal effects in the thermograms was $\pm 1°$ and $\pm 0.5\%$, respectively.

The heat capacity was measured on a DSC-30 unit of a TA-4000 thermoanalyzer, which is a differential scanning calorimeter operating in the temperature scanning mode and designed for quantitative thermal measurements. The heat capacity was determined with a relative error of 2—3%. The systematic measurement error was estimated by determining the thermal capacities of well-studied compounds at regular intervals. The deviations of the measured heat capacities of corundum from the values reported by the National Bureau of Standards (NBS) were ±1—2%.

X-ray powder diffraction analysis was carried out on an FR-552 monochromator chamber (Cu-Kα_1 radiation) using germanium as the internal standard (X-ray diffraction patterns were processed on a IZA-2 comparator with an accuracy of ±0.01 mm) and with the use of the STOE Powder Diffraction System.

Poly[(μ_3-hydroxy)(η^2,μ_3-trimethylacetato-*O*,*O*,*O*′,*O*′)tris(μ_3-trimethylacetato-*O*,*O*,*O*′)(η^2,μ_2-trimethylacetato-*O*,*O*,*O*′)tris(μ_2-trimethylacetato-*O*,*O*′)(μ_2-chloro)(η^1-aquo)(η^1-acetonitrile)(η^1-trimethylacetic acid)pentamanganese(II)], solvate with acetonitrile, {(MeCN)(HOOCBu^t)(H_2O)Mn_5Cl(OH)(OOCBu^t)$_8$·MeCN}$_n$, (4**·MeCN).** Weighed samples of $MnCl_2\cdot 4H_2O$ (0.5 g, 2.53 mmol) and KOOCBu^t (0.47 g, 3.37 mmol) in EtOH (20 mL) were stirred at 80 °C for 1 h. The solution was filtered and concentrated to dryness. Acetonitrile (30 mL) was added to the dry reaction product, and the reaction mixture was stirred at 80 °C for 2 h. The solution was filtered off, concentrated to 15 mL, and kept at 10 °C for 48 h. Colorless crystals of complex **4**·MeCN suitable for X-ray diffraction study were separated from the solution by decantation, washed with cold MeCN (0 °C), and dried under a stream of argon. The yield was 0.31 g (46%). Found (%): C, 44.1; H, 6.7; N, 2.2. $C_{49}H_{90}ClMn_5N_2O_{20}$. Calculated (%): C, 44.01; H, 6.78; N, 2.09. IR (KBr), ν/cm^{-1}: 3440 br.m, 2960 s, 2932 m, 2868 m, 1652 m, 1580 s, 1560 s, 1536 s, 1512 s, 1484 s, 1460 m, 1424 s, 1376 s, 1360 s, 1228 s, 1032 w, 9400 v.s, 896 m, 792 m, 716 v.s, 604 m, 552 w, 416 m.

Poly[bis(η^2,μ_3-trimethylacetato-*O*,*O*,*O*′,*O*′)(μ_3-trimethylacetato-*O*,*O*,*O*′)pentakis(μ_2-trimethylacetato-*O*,*O*′)(μ_2-trimethylacetic acid)(η^1-trimethylacetic acid)tetramanganese(II)], [Mn_4(OOCBu^t)$_8$(HOOCBu^t)$_2$]$_n$ (5). Hexane (or MeCN) (15 mL) was added to a mixture of compound **1** (0.4 g, 1.32 mmol) and HOOCBu^t (0.27 g, 2.6 mmol). The reaction mixture was stirred at 65 °C for 30 min. The colorless solution was concentrated to 7 mL and kept at 20 °C for 48 h. Colorless crystals of complex **5** suitable for X-ray diffraction study were separated from the solution by decantation, washed with cold hexane (0 °C), and dried under a stream of argon. The yield was 0.31 g (76%). Found (%): C, 48.7; H, 7.2. $C_{50}H_{90}Mn_4O_{20}$. Calculated (%): C, 48.79; H, 7.37. IR (KBr), ν/cm^{-1}: 2964 s, 2908 m, 2872 m, 1688 m, 1588 s, 1520 w, 1484 s, 1456 m, 1424 m, 1408 m, 1360 m, 1320 w, 1224 s, 1208 s, 1032 w, 940 w, 900 m, 872 w, 788 m, 768 w, 600 m, 568 w, 536 m, 408 m.

Bis(η^1-trimethylacetato)tetrakis(η^1-trimethylacetic acid)iron(II), Fe(η^1-HOOCBu^t)$_4$(η^1-OOCBu^t)$_2$ (6). ***A.*** A soluion of HOOCBu^t (0.5 g, 4.9 mmol) in hexane (15 mL) was added to **7**·2EtOH (0.26 g, 0.22 mmol). The reaction mixture was stirred at 65 °C for 20 min until a colorless solution was obtained. Then the solution was concentrated to 4 mL and kept at 10 °C for 24 h. Colorless crystals of complex **6** suitable for X-ray diffraction study were separated from the solution by decantation, washed with cold hexane (0 °C), and dried under a stream of argon. The yield was 0.41 g (72%). Found (%): C, 54.0; H, 8.6. $C_{30}H_{58}FeO_{12}$. Calculated (%): C, 54.03; H, 8.77. IR (KBr), ν/cm^{-1}: 2968 s, 2928 m, 2868 m, 1696 s, 1592 s, 1536 w, 1484 s, 1456 m, 1424 s, 1376 m, 1364 m, 1316 w, 1228 s, 1208 m, 1092 v.s, 1032 w, 940 v.s, 900 w, 876 w, 788 w, 764 v.s, 716 w, 604 m, 540 w, 436 m.

B. A solution of HOOCBu^t (0.20 g, 2.0 mmol) in hexane (10 mL) was added to compound **3** (0.10 g, 0.39 mmol). The reaction mixture was stirred at 65 °C for 1 h until a colorless solution was obtained. Then the solution was concentrated to 3 mL and kept at 10 °C for 24 h. Colorless crystals of complex **3** suitable for X-ray diffraction study were separated from the solution by decantation, washed with cold hexane (0 °C), and dried under a stream of argon. The yield was 0.20 g (76%). Found (%): C, 53.9; H, 8.5. $C_{30}H_{58}FeO_{12}$. Calculated (%):

C, 54.03; H, 8.77. IR (KBr), ν/cm^{-1}: 2968 s, 2928 m, 2868 m, 1696 s, 1592 s, 1536 w, 1484 s, 1456 m, 1424 s, 1376 m, 1364 m, 1316 w, 1228 s, 1208 m, 1092 v.s, 1032 w, 940 v.s, 900 w, 876 w, 788 w, 764 v.s, 716 w, 604 m, 540 w, 436 m.

Poly[hexakis(μ$_2$-trimethylacetato-*O*,*O*′)(η^2-1,2-phenylenediamine-*N*,*N*′)triiron(II)], solvate with acetonitrile, {[(η^2-(NH$_2$)$_2$C$_6$H$_4$)$_2$Fe(μ-OOCBu^t)$_2$][Fe$_2$(μ-OOCBu^t)$_4$]·2MeCN}$_n$, (11·2MeCN). A solution of 1,2-phenylenediamine (0.025 g, 0.25 mmol) in MeCN (20 mL) was added to compound **3** (0.09 g, 0.35 mmol), and the reaction mixture was stirred at 80 °C for 30 min. Then the solution was concentrated to 10 mL at 60 °C and kept at room temperature for two days. Colorless crystals of complex **11**·2MeCN suitable for X-ray diffraction study were separated from the solution by decantation, washed with cold MeCN (0 °C), and dried under a stream of argon. The yield was 0.10 g (80%). Found (%): C, 51.8; H, 7.3; N, 7.4. $C_{46}H_{76}Fe_3N_6O_{12}$. Calculated (%): C, 51.48; H, 7.14; N, 7.83. IR (KBr), ν/cm^{-1}: 3358 m, 3284 m, 2960 s, 2924 s, 2872 m, 1584 s, 1552 m, 1532 m, 1484 s, 1456 m, 1429 s, 1376 m, 1360 m, 1280 w, 1224 m, 1064 w, 1032 m, 940 w, 896 w, 856 w, 844 w, 788 m, 744 w, 716 w, 604 m, 532 w, 432 m.

Bis(η^1-trimethylacetato)tetrakis(η^1-1,2-phenylenediamine-*N*)iron(II), Fe(η^1-(NH$_2$)$_2$C$_6$H$_4$)$_4$(η^1-OOCBu^t)$_2$ (12). The complex **7**·2EtOH (0.14 g, 0.12 mmol) and 1,2-phenylenediamine (0.2 g, 1.85 mmol) in EtOH (10 mL) were stirred at 80 °C for 30 min. The resulting colorless solution was concentrated to 3 mL and kept at 10 °C for 24 h. Colorless crystals of complex **12** suitable for X-ray diffraction study were separated from the solution by decantation, washed with cold EtOH (0 °C), and dried under a stream of argon. The yield was 0.13 g (40%). Found (%): C, 59.3; H, 7.4; N, 16.4. $C_{34}H_{50}FeN_8O_4$. Calculated (%): C, 59.10; H, 7.30; N, 16.23. IR (KBr), ν/cm^{-1}: 3544 m, 3388 s, 3364 s, 3320 s, 3252 m, 2960 s, 2928 m, 2868 m, 1620 s, 1600 s, 1532 s, 1500 s, 1476 m, 1464 m, 1412 m, 1372 m, 1356 m, 1276 m, 1224 w, 1148 v.s, 1128 v.s, 1076 w, 1016 s, 928 v.s, 920 v.s, 888 w, 856 m, 796 m, 744 s, 596 m, 516 v.s, 464 m, 440 w, 408 w.

Bis(η^1-trimethylacetato)(η^2-4,5-dimethyl-1,2-phenylenediamine-*N*,*N*′)bis(η^1-4,5-dimethyl-1,2-phenylenediamine-*N*)iron(II), Fe(η^2-(NH$_2$)$_2$C$_6$H$_2$Me$_2$)(η^1-(NH$_2$)$_2$C$_6$H$_2$Me$_2$)$_2$(η^1-OOCBu^t)$_2$ (13). A mixture of the complex **7**·2EtOH (0.2 g, 0.17 mmol) and 4,5-dimethyl-1,2-phenylenediamine (0.27 g, 2.0 mmol) in EtOH (10 mL) was stirred at 80 °C for 30 min. The resulting pale-brown solution was concentrated to 5 mL and kept at 10 °C for 24 h. Colorless crystals of complex **13** suitable for X-ray diffraction study were separated from the solution by decantation, washed with cold EtOH (0 °C), and dried under a stream of argon. The yield was 0.27 g (61%). Found (%): C, 61.3; H, 8.0; N, 12.7. $C_{34}H_{54}FeN_6O_4$. Calculated (%): C, 61.23; H, 8.17; N, 12.61. IR (KBr), ν/cm^{-1}: 3548 m, 3488 s, 3416 s, 3324 s, 3232 m, 2960 s, 2928 m, 2864 m, 1616 s, 1588 s, 1552 m, 1516 s, 1480 m, 1456 w, 1404 m, 1360 m, 1352 m, 1300 w, 1260 v.s, 1224 m, 1092 v.s, 1020 w, 984 m, 884 w, 860 w, 828 v.s, 792 w, 716 v.s, 600 m, 552 v.s, 424 w, 408 w.

X-ray diffraction study of complexes 4—6 and 11—13. X-ray diffraction studies were carried out at the X-ray Structural Center (A. N. Nesmeyanov Institute of Organoelement Compounds of the Russian Academy of Sciences) on a Bruker AXS SMART 1000 diffractometer[22—24] equipped with a CCD detector (λMo, graphite monochromator, 110 K, ω scanning technique with a step of 0.3°, exposure time per frame was 30 s).

The structures of all complexes were solved by direct methods and refined by the full-matrix least-squares method with anisotropic displacement parameters for all nonhydrogen atoms. The hydrogen atoms of the *tert*-butyl substituents of the pivalate ligands as well as the hydrogen atoms of the Me groups and the phenylene fragments of *o*-phenylenediamines were calculated geometrically and refined using a riding model. The protons of the hydroxo groups of the coordinated trimethylacetic acid molecules and the amino groups of the diamine ligands were found in difference Fourier maps and refined isotropically. All calculations were performed with the use of the SHELX97 program package.[26] Crystallographic parameters and structure refinement details are given in Table 1.

This study was financially supported by the Russian Foundation for Basic Research (Project Nos 04-03-32880, 04-03-32883, 05-03-32767, 05-03-32794, and 05-03-08203), INTAS (Grant 03-51-4532), the US Civilian Research and Development Foundation (CRDF, Grant Y1-C-08-12), and the Russian Academy of Sciences (Target Program for Basic Research of the Division of Chemistry and Materials Science of the Russian Academy of Sciences "Chemistry and Physical Chemistry of Supramolecular Systems and Atomic Clusters" and the Program of the Presidium of the Russian Academy of Sciences "Molecular Design of Magnetoactive Compounds and Materials (Molecular Magnets)").

References

1. B. Singh, J. R. Long, F. F. de Biani, D. Gatteschi, and P. Stavropoulos, *J. Am. Chem. Soc.*, 1997, **119**, 7030.
2. W. Wang, C. Ma, X. Zhang, C. Chen, Q. Liu, F. Chen, D. Liao, and L. Li, *Bull. Chem. Soc. Jpn*, 2002, **75**, 2609.
3. A. J. Tasiopoulos, N. C. Harden, K. A. Abboud, and G. Christou, *Polyhedron*, 2003, **22**, 133.
4. P. Christian, G. Rajaraman, A. Harrison, M. Helliwell, J. J. W. McDouall, J. Raftery, and R. E. P. Winpenny, *Dalton Trans.*, 2004, 2550.
5. D. Huang, W. Wang, X. Zhang, C. Chen, F. Chen, Q. Lui, D. Liao, L. Li, and L. Sun, *Eur. J. Inorg. Chem.*, 2004, 1454.
6. M. A. Kiskin, I. G. Fomina, G. G. Aleksandrov, A. A. Sidorov, V. N. Novotortsev, Y. V. Rakitin, Z. V. Dobrohotova, V. N. Ikorskii, Y. G. Shvedenkov, I. L. Eremenko, and I. I. Moiseev, *Inorg. Chem. Commun.*, 2005, **8**, 89.
7. I. L. Eremenko, M. A. Kiskin, I. G. Fomina, A. A. Sidorov, G. G. Aleksandrov, V. N. Ikorskii, Yu. G. Shvedenkov, Yu. V. Rakitin, and V. M. Novotortsev, *J. Cluster Sci.*, 2005, **16**, 331.
8. M. A. Kiskin, Ph. D. (Chem.) Thesis, N. S. Kurnakov Institute of General and Inorganic Chemistry, Russian Academy of Sciences, Moscow, 2005 (in Russian).
9. V. N. Novotortsev, Y. V. Rakitin, V. N. Ikorskii, and I. L. Eremenko, *Mendeleev Commun.*, 2006, **1**.
10. Yu. V. Rakitin, V. M. Novotortsev, V. N. Ikorskii, and I. L. Eremenko, *Izv. Akad. Nauk, Ser. Khim.*, 2004, 2035 [*Russ. Chem. Bull., Int. Ed.*, 2004, **53**, 2124].
11. A. E. Malkov, G. G. Aleksandrov, V. N. Ikorskii, A. A. Sidorov, I. G. Fomina, S. E. Nefedov, V. M. Novotortsev,

I. L. Eremenko, and I. I. Moiseev, *Koord. Khim.,* 2001, **27**, 636 [*Russ. J. Coord. Chem.*, 2001, **27** (Engl. Transl.)].
12. K. R. Maxcy, R. Smith, R. D. Willett, and A. Vij, *Acta Crystallogr., Sect. C: Cryst. Struct. Commun.*, 2000, **56**, e454.
13. A. E. Malkov, I. G. Fomina, A. A. Sidorov, G. G. Aleksandrov, V. N. Ikorskii, V. M. Novotortsev, and I. L. Eremenko, *Izv. Akad. Nauk, Ser. Khim.*, 2003, 489 [*Russ. Chem. Bull., Int. Ed.*, 2003, **52**].
14. S.-M. Peng, C.-T. Chen, D.-S. Liaw, C.-I Chen, and Y. Wang, *Inorg. Chim. Acta*, 1985, **101**, L31.
15. D. Herebian, E. Bothe, F. Neese, T. Weyhermuller, and K. Wieghardt, *J. Am. Chem. Soc.*, 2003, **125**, 9116.
16. E. Bill, E. Bothe, P. Chaudhuri, K. Chlopek, D. Herebian, S. Kokatam, K. Ray, T. Weyhermuller, F. Neese, and K. Wieghardt, *Chem. Eur. J.*, 2005, **11**, 204.
17. A. V. Reshetnikov, A. A. Sidorov, S. S. Talismanov, G. G. Aleksandrov, Yu. A. Ustynyuk, S. E. Nefedov, I. L. Eremenko, and I. I. Moiseev, *Izv. Akad. Nauk, Ser. Khim.*, 2000, 1794 [*Russ. Chem. Bull., Int. Ed.*, 2000, **49**, 1771].
18. I. G. Fomina, A. A. Sidorov, G. G. Aleksandrov, V. N. Ikorskii, V. M. Novotortsev, S. E. Nefedov, and I. L. Eremenko, *Izv. Akad. Nauk, Ser. Khim.*, 2002, 1453 [*Russ. Chem. Bull., Int. Ed.*, 2002, **51**, 1581].
19. I. V. Ovcharenko, Yu. G. Shvedenkov, R. N. Musin, and V. N. Ikorskii, *Zh. Strukt. Khim.,* 1999, **40**, 36 [*Russ. J. Struct. Chem.*, 1999, **40** (Engl. Transl.)].
20. S. Yoon and S. J. Lippard, *Inorg. Chem.*, 2003, **42**, 8606.
21. Yu. V. Rakitin and V. T. Kalinnikov, *Sovremennaya magnetokhimiya* [*Modern Magnetochemistry*], Nauka, St. Petersburg, 1994, 272 (in Russian).
22. *SMART (Control) and SAINT (Integration) Software, Version 5.0*, Bruker AXS Inc., Madison (WI), 1997.
23. G. M. Sheldrick, *SADABS, Program for Scanning and Correction of Area Detector Data*, Göttingen University, Göttinngen (Germany), 1997.
24. G. M. Sheldrick, SHELX97, *Program for the Solution of Crystal Structures*, Göttingen University, Götinngen (Germany), 1997.

Received January 18, 2006;
in revised form April 13, 2006